

Effect of Moderate Hypercapnic Hypoxia on Cerebral Dopaminergic Activity and Brain O₂ Uptake in Intrauterine Growth-Restricted Newborn Piglets

REINHARD BAUER, BERND WALTER, GERD VORWIEGER, ANNE FRITZ, FRANK FÜCHTNER, ULRICH ZWIENER, AND PETER BRUST

Institute of Pathophysiology and Pathobiochemistry [R.B., B.W., G.V., A.F., U.Z.], Universitätsklinikum Jena, Friedrich Schiller University, D-07740 Jena, Germany; Institute of Bioinorganic and Radiopharmaceutical Chemistry [F.F.], Research Center Rossendorf, D-01314 Dresden, Germany; and Institute for Interdisciplinary Isotope Research [P.B.], University Leipzig, D-04318 Leipzig, Germany

ABSTRACT

There is evidence that intrauterine growth restriction (IUGR) is associated with altered dopaminergic function in the immature brain. Compelling evidence exists that in the newborn brain, specific structures are especially vulnerable to O₂ deprivation. The dopaminergic system is shown to be sensitive to O₂ deprivation in the immature brain. However, the respective enzyme activities have not been measured in the living neonatal brain after IUGR under hypercapnic hypoxia (H/H). Therefore, ¹⁸F-labeled 6-fluoro-L-3,4-dihydroxyphenylalanine (FDOPA) together with positron emission tomography was used to estimate the aromatic amino acid decarboxylase activity of the brain of seven normal weight (body weight 2078 ± 434 g) and seven IUGR newborn piglets (body weight 893 ± 109 g). Two positron emission tomography scans were performed in each piglet. All animals underwent a period of normoxia and moderate H/H. Simultaneously, cerebral blood flow was measured with colored microspheres and cerebral metabolic rate of O₂ was determined. In newborn normal-weight piglets, the rate constant for FDOPA decarboxylation was markedly increased in mesostriatal regions during H/H, whereas brain oxidative metabolism remained unaltered. In contrast, moderate H/H induced in IUGR piglets a marked reduction of clearance rates for FDOPA metabolites ($p < 0.05$), which was accompanied by a tendency of lowering the rate constant for FDOPA conversion. Furthermore, IUGR piglets maintained cerebral O₂ uptake in the early period of H/H, but during the late period of H/H, a significantly reduced cerebral

metabolic rate of O₂ occurred ($p < 0.05$). Thus, IUGR is accompanied by a missing activation of dopaminergic activity and attenuated brain oxidative metabolism during moderate H/H. This may indicate endogenous brain protection against O₂ deprivation. (*Pediatr Res* 57: 363–370, 2005)

Abbreviations

AADC, aromatic amino acid decarboxylase
ADHD, attention-deficit/hyperactivity disorder
CBF, cerebral blood flow
CMRO₂, cerebral metabolic rate of O₂
CVR, cerebrovascular resistance
DA, dopamine
FDA, fluorodopamine
FDOPA, ¹⁸F-labeled 6-fluoro-L-3,4-dihydroxyphenylalanine
H/H, hypercapnic hypoxia
IUGR, intrauterine growth restriction
K₁^{FDOPA}, unidirectional clearance of FDOPA
k₂^{FDOPA}, regional rate constant for FDOPA backflux from the brain
k₃^{FDOPA}, apparent AADC activity
k_{cl}^{FDA+acids}, clearance rate constant for FDOPA metabolites
MAP, mean arterial blood pressure
PET, positron emission tomography
PS^{FDOPA}, permeability-surface area product of FDOPA

Intrauterine growth restriction (IUGR) is still an unresolved problem in perinatal medicine. Perinatal mortality is increased

after IUGR (1,2), as well as the incidence of perinatal asphyxia, because placental insufficiency is the main cause of IUGR (3) in developed countries.

The consequences of severe hypercapnic hypoxia (H/H) combined with brain ischemia, mostly as a result of secondary hypotension (4), are well documented to be associated with neuronal damage as a frequent cause of the chronic handicapping conditions of cerebral palsy, mental retardation, and epilepsy (5). Compelling evidence exists that in the newborn

Received April 27, 2004; accepted August 2, 2004.

Correspondence: Reinhard Bauer, M.D., Ph.D., Institute for Pathophysiology and Pathobiochemistry Universitätsklinikum Jena, Friedrich Schiller University, D-07740 Jena, Germany; e-mail: Reinhard.Bauer@mti.uni-jena.de

Supported by the Thuringian State Ministry of Science, Research, and Arts, Grant 3/95-13 (R.B.) and the Saxon Ministry of Science and Art, Grant 7541.82-FZR/309 (P.B.).

DOI: 10.1203/01.PDR.0000150800.19956.F0

brain, specific structures and/or tissues are especially vulnerable to injury, creating syndromes of functional disabilities. In term newborns, a specific pattern of symmetric basal ganglia and adjacent cortex injury has been revealed as the structural substrate for extrapyramidal cerebral palsy (6–8). It has been proposed that neurons that are connected in already established neuronal circuits seem to be especially vulnerable to excitotoxic damage based on a hyperactivity of the major excitatory glutamatergic input (9). However, the dopaminergic system is also sensitive to O₂ deprivation in the immature brain (10–12). Obviously, there is no “oxygen reserve” that protects dopamine (DA) release and metabolism from decrease in O₂ pressure, because in the newborn piglet brain, even a small reduction of the brain tissue Po₂ causes a significant increase in the striatal extracellular DA concentration in a dose-dependent relationship (13). We showed previously that H/H induces an increase of aromatic amino acid decarboxylase (AADC) activity, indicating an increase of mesostriatal dopaminergic activity in newborn piglets (14), which is known to be associated with pronounced neuronal injury as a result of hypoxic-ischemic brain (15,16).

It is interesting that IUGR is also associated with an up-regulation in metabolic activity of the mesostriatal and telencephalic dopaminergic system that was not related to alterations in brain oxidative metabolism (17). However, until now, the effect of O₂ deprivation on brain DA metabolism was not determined. Therefore, we estimated the activity of AADC, the ultimate enzyme in DA synthesis, in the brain regions of the mesostriatal and telencephalic dopaminergic system together with measurements of cerebral blood flow (CBF) and cerebral metabolic rate of O₂ (CMRO₂) under normoxic conditions and during moderate H/H in normal-weight and IUGR newborn piglets. We asked whether moderate H/H induces a reinforcement of the already elevated dopaminergic activity in IUGR newborn piglets. We used a morphometrically well-characterized state of asymmetric IUGR in newborn piglets (18) and included animals with optimal vital conditions early after birth.

METHODS

Animals. All surgical and experimental procedures were approved by the committee of the Saxon State government on animal research. Animals were obtained from a breeding farm. Delivery was observed, and the viability of neonatal piglets was assessed immediately after birth so that only animals with a viability score ≥ 7 (19) were included in the study. Immediately before the onset of the experiments, animals were carried to the laboratory in a climatized transport incubator (environmental temperature 33–34°C; time for transportation 30–60 min). Animals were divided into normal-weight piglets ($n = 7$; aged 3–5 d; body weight 2078 ± 434 g) and IUGR piglets ($n = 7$; aged 2–5 d; body weight 893 ± 109 g) according to their birth weight. The birth weight distribution of the breed of piglets used here (German Landrace) has been described previously (18).

Anesthesia and surgical preparation. The piglets were initially anesthetized with 2.5% isoflurane in 70% nitrous oxide and 30% O₂ by mask. The anesthesia was maintained throughout the surgical procedure with 0.8% isoflurane. A central venous catheter was introduced through the left external jugular vein and was used for the administration of drugs and for volume substitution (lactated Ringer's solution: 5 mL/h). An endotracheal tube was inserted through a tracheotomy. After immobilization with pancuronium bromide ($0.2 \text{ mg} \cdot \text{kg body weight}^{-1} \cdot \text{h}^{-1}$, i.v.), the piglets were artificially ventilated (Servo Ventilator 900C; Siemens-Elema, Solna, Sweden). The artificial ventilation was adjusted to maintain normoxic and normocapnic blood gas values. Polyurethane catheters (inner diameter 0.8 mm) were advanced through both umbilical arteries into the abdominal aorta to record the MAP and to withdraw reference samples for the colored microsphere technique. An additional poly-

urethane catheter (inner diameter 0.3 mm) was inserted into the superior sagittal sinus through a midline burr hole (3 mm in diameter and located 4 mm caudal to the bregma) and advanced to the confluence sinuum to obtain brain venous blood samples. The left ventricle was cannulated retrogradely via the right common carotid artery with a polyurethane catheter (inner diameter 0.5 mm). An arterial, the left ventricular, and the central venous catheters were connected with pressure transducers (P23Db; Statham Instruments, Hato Rey, Puerto Rico). Correct positioning of the catheter tips was checked by continuous pressure trace recordings and by autopsy at the end of the experiment. Body temperature was monitored by a rectal temperature probe and was maintained throughout the general instrumentation at $38 \pm 0.3^\circ\text{C}$ using a warmed pad and a feedback-controlled heating lamp. Physiologic parameters were recorded on a multichannel polygraph (Gould Nicolet Messtechnik GmbH, Erlensee, Germany). MAP was monitored continuously, and arterial blood samples were withdrawn and analyzed at regular intervals to monitor blood gases and whole-blood acid-base parameters.

Experimental protocol. After the surgical preparation had been completed, the anesthesia was reduced to 0.25% isoflurane in 65% nitrous oxide and 35% O₂ and the piglets were allowed to stabilize for 1 h. The piglets were studied lying prone in a positron emission tomography (PET) scanner with the head in a custom-made head holder. The position of the head was checked throughout the experiment with laser markers.

Two PET studies were performed in each animal. The first PET study was done under normoxic/normocapnic conditions in both groups; 8 h later, a second PET study was performed under conditions of moderate H/H. Therefore, animals underwent in the second part of the experiment a change in their inspired gas composition (fraction of inspired O₂ was lowered from 0.35 to 0.09 in exchange for nitrogen, and CO₂ was added resulting in an arterial Pco₂ between 72 and 76 mm Hg). The second PET study was started 20 min after H/H was introduced. Blood volume replacement was given after each blood withdrawal using stored heparinized blood obtained from donor sibling piglets.

Measurements. The regional CBF was measured by means of the reference sample color-labeled microsphere (Dye-Trak; Triton Technology, San Diego, CA) technique, which represents a valid alternative to the radionuclide-labeled microsphere method for organ blood flow measurement in newborn piglets without the disadvantages arising from radioactive labeling with long-lived isotopes (20). Application of this technique in piglets and methodical considerations have been presented and discussed in detail elsewhere (20,21). Briefly, in random sequence between 900,000 and 1.2 million colored polystyrene microspheres were injected into the left ventricle. A blood sample was withdrawn from the thoracic aorta as the reference sample. The injection line then was flushed with 2 mL of saline. A blood sample was withdrawn from the abdominal aorta as the reference sample (22), beginning 15 s before the microsphere injection and continuing for 2 min at a rate of 1.50 mL/min (syringe pump SP210iw; World Precision Instruments, Sarasota, FL). At the end of each experiment, the brains were removed and sectioned in the desired brain regions. For digestion, reference blood samples and tissue samples between 0.5 and 2.5 g were covered with an appropriate volume ($\sim 3 \text{ mL/g}$) of digestive solution (4 N of KOH with 4% Tween 80 in deionized water). All tissue and blood samples were digested for a minimum of 4 h at 60°C. For isolating the microspheres, each tissue sample was digested and then filtered under vacuum suction through an 8- μm pore polyester-membrane filter. Colored microspheres were quantified by their dye content. The dye was recovered from the microspheres by adding dimethylformamide. The photometric absorption of each dye solution was measured by a diode-array UV/visible spectrophotometer (Model 7500; Beckman Instruments, Fullerton, CA). Calculations were performed using the MISS software (Triton Technology). The number of microspheres was calculated using the specific absorbance value of the different dyes. All reference and tissue samples contained >400 microspheres.

The heart rate, arterial blood pressure, arterial and brain venous pH, Pco₂, Po₂, O₂ saturation, and Hb values were measured immediately before the microsphere injection. Blood pH, Pco₂, and Po₂ were measured with a blood gas analyzer (model ABL50; Radiometer, Copenhagen, Denmark), and blood Hb and O₂ saturation were measured using a hemoximeter (model OSM2; Radiometer) and corrected to the body temperature of the animal at the time of sampling.

The absolute flows to the tissues measured by the colored microspheres were calculated by the formula $\text{flow}_{\text{tissue}} = \text{number of microspheres}_{\text{tissue}} \times (\text{flow}_{\text{reference}} / \text{number of microspheres}_{\text{reference}})$. Flows are expressed in milliliters per minute per 100 g of tissue by normalizing for tissue weight. Blood O₂ content (cO₂) was calculated using the equation $\text{cO}_2 [\text{mL/dL}] = \text{cHb} [\text{g/dL}] \times \text{sO}_2 [\text{mmol/mmol}] \times 1.39 [\text{mL/g}] + (\text{Po}_2 [\text{mm Hg}] \times \alpha \text{O}_2 [\text{mL} \cdot \text{dL}^{-1} \cdot \text{mm Hg}^{-1}])$ to obtain the sum of O₂ that is physically dissolved and chemically bound to Hb, where cHb is Hb concentration, sO₂ is O₂ saturation, 1.39 (mL/g) is the theoretical O₂ capacity of Hb, and αO_2 is the solubility of O₂ in blood [$\text{cHb} \times 0.000054$ (Hb-dependent O₂ solubility) + 0.0029 (solubility of O₂ in

plasma)]. Because the sagittal sinus drains the cerebral cortex, the cerebral white matter, and some deep gray structures (basal ganglia, thalamus, and hippocampus) (23), the blood flow measured to the forebrain included these structures. The CMRO₂ was obtained by multiplying the blood flow to the forebrain by the cerebral arteriovenous O₂ content difference. Cerebrovascular resistance (CVR) was calculated by division of MAP by CBF.

PET studies. ¹⁸F-labeled 6-fluoro-L-3,4-dihydroxyphenylalanine (FDOPA) was produced according to the destannylation method by direct fluorination of the tin-precursor with [¹⁸F]F₂ (24) simplifying the procedure [see (25)]. The piglets were studied lying prone in the scanner (CTI/Siemens ECAT EXACT HR+; dynamic scans: 35 frames between 30 and 600 s each, total length 120 min). In each case, 50–150 MBq of FDOPA was infused within 60 s into the upper caval vein, followed immediately by heparinized isotonic saline (1 IU of heparin/mL) to flush the catheter. Fifty-two arterial blood samples were obtained in intervals between 15 s and 30 min, stored on ice, and centrifuged for plasma sampling. Plasma activity (100 μL) was measured in a well counter (COBRA II) cross-calibrated with the tomograph. In addition, nine blood samples (at 2, 4, 8, 12, 16, 25, 50, 90, and 120 min) were withdrawn for HPLC analysis to correct the plasma input function for the presence of FDOPA metabolites (26). PET imaging was performed with an ECAT EXACT HR+ (CTI/Siemens) scanner at a spatial resolution (transaxial) of 4–5 mm (27). Reconstruction of both PET scans was done using filtered back projection with a Hanning filter (cutoff frequency of 0.5). For attenuation and scatter correction, a transmission scan using three rotating ⁶⁸Ge rod sources was performed before the emission scan. Radioactivity data of selected volumes of interest were obtained using a standardized procedure that was recently described in detail (28). Briefly, volumes of interest defined on magnetic resonance images were aligned to the added PET radioactivity images interactively using an “in house” data analysis tool.

The PET data analysis was performed using compartment modeling based on FDOPA models described in humans (29) and described in detail previously (14). Briefly, FDOPA is reversibly transferred across the blood-brain barrier *via* the transport system for large neutral amino acids LAT1, a process described by the rate constants unidirectional clearance of FDOPA (K_1^{FDOPA}) and regional rate constant for FDOPA backflux from the brain (k_2^{FDOPA}) (28). From K_1^{FDOPA} , we estimated the regional permeability-surface area products (PS^{FDOPA}) of the cerebrovascular endothelium.

In the brain, FDOPA is decarboxylated to fluorodopamine (FDA) by AADC at the rate constant apparent AADC activity (k_3^{FDOPA}). FDA is stored in vesicles or further metabolized by the enzymes MAO and COMT, yielding the acidic substances fluoro-dihydroxyphenylacetic acid and fluoro-homovanillic acid. These processes are combined into a single compartment with the clearance rate constant for FDOPA metabolites ($k_{cl}^{FDA+acids}$), which accounts for the clearance of labeled metabolites from tissue. The rate of the conversion from FDA to fluoro-3-methoxytyramine by the enzyme catechol-O-methyltransferase has not to be considered, because only trace amounts of fluoro-3-methoxytyramine are formed in the striatum (30).

The relevant differential equations that describe the changes of radioactivity contents in these compartments are as follows:

$$dM_f^{FDOPA}/dt = K_1^{FDOPA}C_a^{FDOPA}(t) - k_2^{FDOPA}M_f^{FDOPA}(t) - k_3^{FDOPA}M_f^{FDOPA}(t) \quad (1)$$

$$dM_m^{FDOPA}/dt = k_3^{FDOPA}M_f^{FDOPA}(t) - k_{cl}^{FDA+acids}M_m^{FDOPA}(t) \quad (2)$$

where $M_f^{FDOPA}(t)$ is the amount of free FDOPA in the brain and $M_m^{FDOPA}(t)$ is the regional content of FDOPA metabolites.

The rate constants for blood-brain and brain-blood transfer (K_1 and k_2), the apparent AADC activity (k_3^{FDOPA}), and the clearance rate constant ($k_{cl}^{FDA+acids}$) were estimated by solving these differential equations for the measurable variables. As stated by Cumming and Gjedde (30), k_3^{FDOPA} is the fractional rate constant for decarboxylation, defined relative to the enzyme's Michaelis constants ($V_{max}/K_m + [C]$), where $[C]$ is the concentration of L-DOPA, the endogenous substrate, which is much less than K_m (30). The PS product was calculated from K_1 and CBF (F):

$$PS = -F * \ln(1 - K_1/F)$$

Statistical analysis. Data are reported as means ± SD. Comparisons between groups were made with unpaired *t* tests. Comparisons between baseline and PET measurements within the groups were made with paired *t* tests. One-way ANOVA, with repeated measures, was used to compare CBF values and PET data of different brain regions. A Bonferroni adjustment was performed to evaluate significant differences. Differences were considered significant at $p < 0.05$.

RESULTS

In piglets with IUGR, the body weight was greatly reduced (43% of normal-weight group; Table 1). Naturally occurring growth restriction in swine is asymmetrical with an increase in the mean ratio of brain weight to liver weight from 0.64 ± 0.18 to 1.44 ± 0.19 ($p < 0.01$). The reduction in brain weight was small (84% of normal-weight group). In contrast, the decrease in liver weight (36% of normal-weight group) was similar to that in body weight (42% of normal-weight group). All differences in organ weight were significant ($p < 0.01$).

Table 2 summarizes the values for MAP, heart rate, arterial blood gases, acid-base balance, and energy fuels, which were obtained during the blood flow measurements under normoxia and H/H. They cover a time schedule of >8 h. The values measured under normoxic conditions before (control 1; time: 0) and during the first PET study (normoxia; time: +60 min) and before onset of H/H (control 2; time: +8 h) were within the physiologic range in both groups studied and consistent with other data obtained from mildly anesthetized and artificially ventilated newborn piglets (31). Widely unchanged values during the first PET scan measurement and the resting period of ~8 h were also measured for the cerebral hemodynamics and the cerebral O₂ uptake (Fig. 1).

The regional transport of FDOPA to the brain indicated by K_1^{FDOPA} and PS^{FDOPA} and the clearance rate of labeled metabolites from brain tissue ($k_{cl}^{FDA+acids}$) were similar in both groups (Table 3). However, the regional rate constant for backflux (k_2^{FDOPA}) from frontal cortex was markedly increased in piglets with IUGR ($p < 0.05$). Furthermore, the rate constant for FDA production (k_3^{FDOPA}) was markedly increased in all brain regions of piglets with IUGR studied ($p < 0.05$; Fig. 2), indicating a distinct up-regulation of AADC activity. Mesencephalic k_2^{FDOPA} and the frontal cortex k_3^{FDOPA} values were significantly lower compared with the corresponding striatal transfer coefficients in the piglets with IUGR.

The supposed degree of moderate H/H, *i.e.* a reduction of PAO₂ of approximately one third of baseline value in addition to nearly doubling arterial partial pressure of CO₂, led to a significant increase of heart rate ($p < 0.05$) at widely maintained MAP together with combined respiratory and metabolic acidosis and progressively increased plasma lactate content in both animal groups ($p < 0.05$). In addition, a corresponding decrease in arterial O₂ content to approximately one third occurred, resulting in reduced cerebral arteriovenous difference of O₂ ($p < 0.05$; Table 2). Furthermore, during the late period of moderate H/H, an increased cerebral arteriovenous difference of lactate was found in piglets with IUGR ($p < 0.05$).

Table 1. Organ weights of newborn piglets after normal growth or IUGR

	NW piglets (n = 7)	IUGR piglets (n = 7)
Body weight (g)	2078 ± 434	893 ± 109*
Brain weight (g)	36 ± 3	30 ± 1*
Liver weight (g)	60 ± 17	21 ± 3*
Brain/liver ratio	0.64 ± 0.18	1.44 ± 0.19*

Values are means ± SD.

* $p < 0.01$, comparison between normal weight (NW) newborn piglets and piglets with IUGR.

Table 2. Physiologic values for newborn normal-weight piglets ($n = 7$) and piglets with IUGR ($n = 7$) during normoxia (1st PET) and H/H (2nd PET)

	Control 1	1 st PET	Control 2	2 nd PET 1	2 nd PET 2
MAP (mm Hg)					
NW	75 ± 13	79 ± 14	69 ± 11	77 ± 10	74 ± 13
IUGR	69 ± 11	68 ± 14	65 ± 7	71 ± 9	54 ± 22
Heart rate (min)					
NW	231 ± 41	221 ± 50	232 ± 43	253 ± 36	267 ± 16†
IUGR	201 ± 41	184 ± 46	207 ± 49	235 ± 15†	223 ± 24*
Arterial Pco ₂ (mm Hg)					
NW	39 ± 2	38 ± 1	37 ± 2	76 ± 4†	75 ± 5†
IUGR	40 ± 3	40 ± 3	39 ± 4	72 ± 4†	72 ± 4†
Arterial pH					
NW	7.44 ± 0.03	7.47 ± 0.03	7.48 ± 0.04	7.15 ± 0.04†	6.99 ± 0.11†
IUGR	7.47 ± 0.03	7.47 ± 0.03	7.48 ± 0.06	7.20 ± 0.04†	7.03 ± 0.14†
Arterial base excess (mmol/L)					
NW	3 ± 2	4 ± 2	5 ± 3	-2 ± 2†	-13 ± 5†
IUGR	5 ± 2	6 ± 2	6 ± 3	-3 ± 3†	-14 ± 9†
Arterial Po ₂ (mm Hg)					
NW	128 ± 26	134 ± 32	124 ± 23	34 ± 5†	40 ± 8†
IUGR	120 ± 19	111 ± 30	120 ± 27	35 ± 4†	41 ± 7†
Arterial oxygen content (mmol/L)					
NW	4.9 ± 1.0	4.9 ± 1.1	4.8 ± 1.1	1.6 ± 0.2†	1.5 ± 0.3†
IUGR	5.8 ± 1.1	5.3 ± 1.1	5.4 ± 1.1	1.8 ± 0.4†	1.7 ± 0.5†
Arterial lactate content (mmol/L)					
NW	2.3 ± 0.8	2.1 ± 0.6	2.1 ± 0.6	5.1 ± 1.7†	13.1 ± 5.5†
IUGR	1.6 ± 0.5	1.9 ± 0.4	2.2 ± 1.2	4.9 ± 2.2†	13.7 ± 6.8†
Cerebral avDO ₂ (mmol/L)					
NW	2.37 ± 0.67	2.83 ± 0.86	2.75 ± 0.81	0.86 ± 0.27†	1.09 ± 0.35†
IUGR	2.84 ± 0.83	2.73 ± 0.71	2.71 ± 0.62	0.98 ± 0.36†	1.20 ± 0.54†
Cerebral avD lactate (mmol/L)					
NW	-0.16 ± 0.46	-0.04 ± 0.29	-0.09 ± 0.25	-0.4 ± 1.19	0.10 ± 0.85
IUGR	0.04 ± 0.10	0.01 ± 0.11	0.03 ± 0.17	0.36 ± 0.50	0.77 ± 0.64†

Values are means ± SD. NW, normal-weight; avD, arterial-brain venous difference.

* $p < 0.05$. * Significant differences between NW and IUGR animals, † significant differences within the related group compared with control 1.

In newborn normal-weight piglets, brain oxidative metabolism obviously has not been compromised throughout the whole period of H/H. A pronounced CBF increase ($p < 0.05$) and a considerable CVR reduction ($p < 0.05$) resulted in an unchanged CMRO₂ (Fig. 1). In contrast, piglets with IUGR maintained cerebral O₂ uptake in the early period of H/H together with an appropriate CVR decrease and corresponding CBF elevation ($p < 0.05$). However, during the late period of H/H, a significantly reduced CMRO₂ occurred, accompanied by a markedly blunted CBF increase ($p < 0.05$; Fig. 1).

During moderate H/H, K_1^{FDOPA} , k_2^{FDOPA} and also the clearance rate constant $k_{\text{cl}}^{\text{FDA+acids}}$ tended to increase in all brain regions of normal-weight piglets and was significant for k_2^{FDOPA} in frontal cortex ($p < 0.05$; Table 3). The PS^{FDOPA} was unchanged. Furthermore, the rate constant for FDOPA decarboxylation (k_3^{FDOPA}) was markedly increased in mesencephalon (84%) and striatum (42%) during H/H ($p < 0.05$; Fig. 2). In contrast, moderate H/H induced in piglets with IUGR a marked reduction of the clearance rate constant $k_{\text{cl}}^{\text{FDA+acids}}$ ($p < 0.05$; Table 3), which was accompanied by a tendency of lowering k_3^{FDOPA} .

DISCUSSION

The main new finding in this study is that moderate H/H does not induce a further increase in DA production within the mesostriatal and telencephalic dopaminergic system of new-

born piglets with IUGR. This finding was in contrast to the response of H/H in normal-weight piglets, in which an increase of the AADC activity within the mesencephalon and striatum has been shown ($p < 0.05$; Fig. 2), which confirms previous data (14). The markedly reduced clearance rates for FDOPA metabolites give further evidence for a compromised DA turnover during H/H in piglets with IUGR ($p < 0.05$; Table 3).

Methodologically, it has been considered that PET study with FDOPA reflects several elements of the dopaminergic neurotransmission, including functional aspects such as enzymatic activities, uptake through the membrane transporter, and vesicular storage as well as anatomic aspects such as the density of dopaminergic nerve endings. Nevertheless, the estimation of AADC activity by compartmental analysis of transport and metabolism of FDOPA in newborn piglets was confirmed previously (14,25). Furthermore, the amount of combined respiratory and metabolic acidosis as well as the estimated cardiovascular effects owing to prolonged H/H were widely similar in newborn normal-weight and IUGR piglets. Therefore, there is no evidence that a comparable amount of systemic load with moderate H/H led to marked differences in the systemic response between normal-weight and IUGR newborns, which may be responsible for the documented differences of cerebral dopaminergic and oxidative metabolism.

The cause for the reported blunted H/H-induced response of AADC activity in newborn piglets with IUGR cannot be found

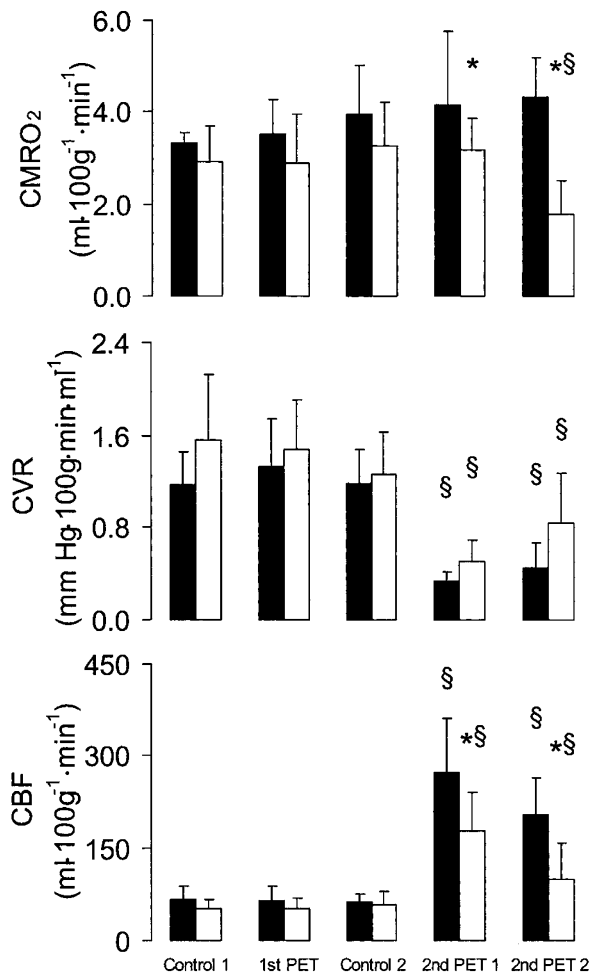


Figure 1. CBF, CVR, and CMRO₂ in newborn normal-weight piglets ($n = 7$; ■) and piglets with IUGR ($n = 7$; □) under normoxic conditions [before (control 1) and during first PET scan procedure (60 min after FDOPA injection)] and just before (control 2) and during moderate hypercapnic hypoxia [during the second PET scan procedure (2nd PET 1 indicates 10 min before; 2nd PET 2 indicates 60 min after FDOPA injection)]. * $p < 0.05$; §significant differences between normal-weight piglets and piglets with IUGR; §significant differences within the related group compared with control 1.

in the recent study. Nevertheless, the combined respiratory and metabolic acidosis induced by moderate H/H seems not to be responsible for any alterations of blood-brain transport of [¹⁸F]FDOPA. Whereas influx data from normal-weight piglets showed no differences between normal conditions and H/H, there was a tendency of improved tracer exchange during H/H in animals with IUGR ($p < 0.05$; Table 3). Furthermore, the PS^{FDOPA} in striatum and mesencephalon was increased in animals with IUGR during H/H. Hence, the absence of AADC increase in piglets with IUGR is obviously not induced by insufficient substrate influx during H/H.

The functional relevance of altered AADC during H/H in piglets with IUGR remains speculative. It is now established that AADC represents an additional important regulated step in the synthesis of DA (32). Accumulated evidence suggests that the AADC activity in the adult brain is modulated by short- and long-term mechanisms that seem to involve enzyme activation and induction. DA itself is able to modulate AADC activity (33–35). However, because AADC seems to be present in a

large excess for neurotransmitter synthesis in dopaminergic neurons, effects of AADC regulation are suggested not to be predominantly relevant for the control of the overall flux in this pathway. The reduced clearance rates for FDOPA metabolites suggest a reduced DA turnover during H/H in piglets with IUGR. Tyrosine hydroxylase is proposed to catalyze the rate-limiting step of DA synthesis in the brain. A previous study showed a dose-dependent response of O₂ deprivation on tyrosine hydroxylase activity in the newborn piglet striatum. Indeed, an increased activity was reported during mild reduction of brain tissue Po₂ but a proportional decrease of the enzyme activity during moderate H/H (36). The latter finding confirms reports obtained from rats that the first rate-limiting step in the synthesis of the monoamine neurotransmitters DA, noradrenaline, and 5-hydroxy-tryptophan is affected during moderate as well as severe hypoxia at all stages of development (37). Furthermore, the reduced catabolism of DA by monoamine oxidase could be responsible for reduced clearance rates for FDOPA metabolites in piglets with IUGR during moderate H/H. Hypoxia caused a substantial decrease in the levels of 3,4-dihydroxyphenylacetic acid and homovanillic acid, two key metabolites of DA degradation in newborn piglet brain during severe hypoxic hypoxia (38).

Even if the causal relationship between IUGR and altered dopaminergic activity remains unsolved, their consequences on vulnerability of dopaminergic brain structures as a result of O₂ deprivation are relevant to be discussed. In newborn piglets, it has been shown that O₂ deprivation responds with gradual increase of [DA]_e as a result of reduced brain tissue Po₂ in a dose-dependent manner (13). The hypothesis that an increase of [DA]_e during a hypoxic insult plays an important role in the pathogenesis of neuronal injury in newborn brain is supported by numerous findings from different injury models. DA obviously plays an important role in ischemia-reperfusion injury, because it has been suggested that an increase in extracellular DA can result in alterations in the sensitivity of neurons to excitatory amino acids (39). Therefore, the reduced DA turnover, indicated by slightly diminished AADC activity and reduced clearance rates for FDOPA metabolites in piglets with IUGR during moderate H/H, is suggested to reduce the risk for hypoxia-induced brain injury of dopaminergic brain structures.

There is compelling evidence that the vulnerable mesotelencephalic DA pathways to perinatal mild to moderate O₂ deprivation are associated with long-term impairment of DA signaling and executive functioning (40,41). Recent studies demonstrate that perinatal intermittent hypoxia is sufficient to induce sustained alterations in sleep-wake architecture, locomotor hyperactivity, executive dysfunction, and striatal DA 1 receptor and vesicular monoamine transporter protein immunoreactivity (42). Furthermore, attention-deficit/hyperactivity disorder (ADHD), although largely thought to be a genetic disorder, has environmental factors that seem to contribute significantly to the etiopathogenesis of the disorder. Indeed, in adolescents who have ADHD, high DA receptor availability was predicted by low neonatal CBF, supporting the hypothesis of cerebral ischemia as a contributing factor in infants who are susceptible to ADHD (43).

Table 3. Transfer coefficients and PS^{FDOPA} of different brain regions calculated from the measured tracer activities in arterial blood and brain of newborn piglets during normoxia (1st PET) and H/H (2nd PET) in newborn normal-weight piglets ($n = 7$) and piglets with IUGR ($n = 7$)

Brain region	K_1^{FDOPA} (mL·g ⁻¹ ·min ⁻¹)		k_2^{FDOPA} (min)		$k_{ci}^{FDA+acids}$ (min)		PS^{FDOPA} (mL·g ⁻¹ ·min ⁻¹)	
	NW piglets	IUGR piglets	NW piglets	IUGR piglets	NW piglets	IUGR piglets	NW piglets	IUGR piglets
Mesencephalon								
1 st PET	0.072 ± 0.024	0.061 ± 0.032	0.091 ± 0.051	0.087 ± 0.043§	0.011 ± 0.008	0.015 ± 0.003	0.077 ± 0.026	0.065 ± 0.035
2 nd PET	0.085 ± 0.044	0.074 ± 0.042§	0.115 ± 0.036†	0.103 ± 0.035†	0.015 ± 0.005†	0.008 ± 0.004*†‡	0.086 ± 0.045	0.077 ± 0.045†
Frontal Cortex								
1 st PET	0.064 ± 0.020	0.051 ± 0.019	0.059 ± 0.030	0.098 ± 0.032*	0.003 ± 0.016	0.015 ± 0.007	0.069 ± 0.022	0.054 ± 0.020
2 nd PET	0.076 ± 0.036	0.058 ± 0.035	0.089 ± 0.026‡	0.088 ± 0.021	0.011 ± 0.004	0.005 ± 0.003*‡	0.079 ± 0.040	0.064 ± 0.044
Striatum								
1 st PET	0.069 ± 0.019	0.059 ± 0.023	0.071 ± 0.024	0.124 ± 0.061	0.007 ± 0.010	0.013 ± 0.006	0.075 ± 0.021	0.063 ± 0.025
2 nd PET	0.078 ± 0.038	0.067 ± 0.038§	0.103 ± 0.033	0.094 ± 0.024	0.010 ± 0.003	0.005 ± 0.002*‡	0.080 ± 0.042	0.072 ± 0.046†

Values are means ± SD.

Values are means ± SD; *†‡§ $p < 0.05$; * indicates significant differences between NW and IUGR piglets, ‡ significant differences between 1st and 2nd PET measurement, † significant differences to frontal cortex, § significant differences to striatum.

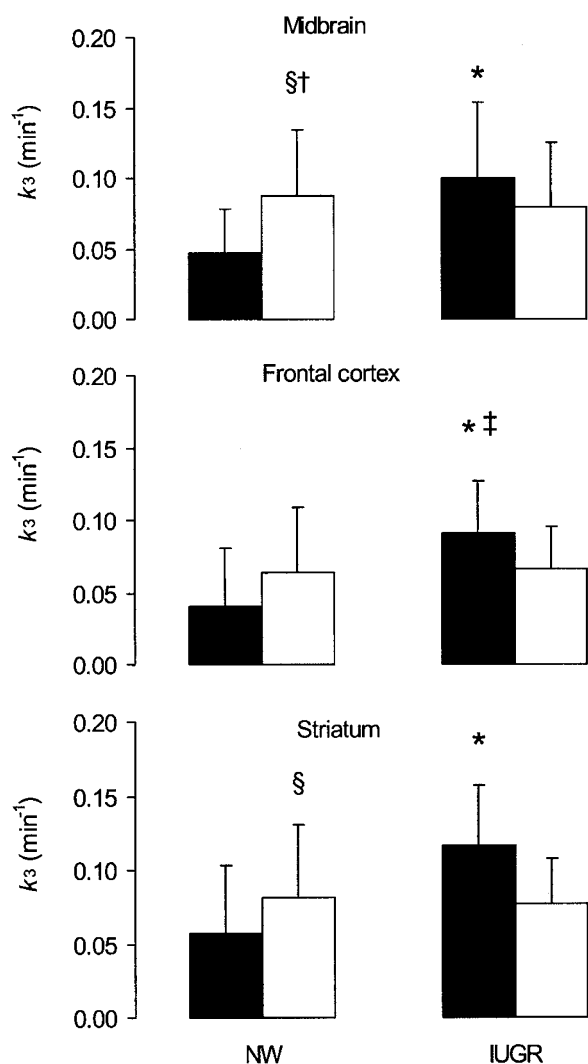


Figure 2. Effect of H/H (□) on rate constants for FDA production (k_3^{FDOPA}) in different brain regions of normal-weight piglets (NW; $n = 7$) and piglets with IUGR (IUGR; $n = 7$), compared with those of NW ($n = 10$). Values are means ± SD; *†‡§ $p < 0.05$; *significant difference between NW and IUGR; §significant differences between first and second PET measurement; †significant differences to frontal cortex; ‡significant differences to striatum.

The quantitative differences in CBF response during H/H between newborn normal-weight piglets and piglets with IUGR suggest an altered cerebrovascular reactivity as a con-

sequence of compromised intrauterine development. Furthermore, the restricted CBF increase of newborn piglets with IUGR seems to involve time-dependently different consequences of cerebral O_2 supply. During the early period of H/H, the restricted CBF increase was sufficient to maintain brain O_2 uptake. Hence, IUGR-associated altered cerebrovascular reactivity seems to improve efficiency of cerebral O_2 uptake. However, during late H/H, a further CBF decrease compared with a mild CVR increase resulted in a marked $CMRO_2$ reduction despite slightly increased cerebral arteriovenous O_2 difference. Underlying mechanisms of altered cerebrovascular reactivity as a result of compromised intrauterine development remain to be elucidated. Only a few data about the effects of IUGR on CBF regulation in neonates are available so far. We showed recently that IUGR resulted in an improved ability of growth-restricted newborn piglets to withstand critical periods of gradual O_2 deficit owing to an improved cerebrovascular autoregulation during hemorrhagic hypotension (44). This response suggested a delayed vasodilatory reaction at gradually reduced cerebral perfusion pressure, which could be provoked by an attenuated generation of vasodilatory factors. Despite a still-limited knowledge of mechanisms that regulate the perinatal cerebrovascular tone (45), some age-related hormonal effects on cerebral smooth muscles seem to be of special importance for a deeper understanding of altered cerebrovascular responses after compromised intrauterine development and/or during disturbed respiratory gas exchange. Synthetic glucocorticoid administration attenuates cerebral vasodilative responses to hypercapnia in newborn piglets (46). This was shown to be mediated by preventing the CO_2 -induced endothelium-derived prostanoid release by cyclooxygenase inhibition and discussed as one of several factors that can be responsible for hypercapnia-induced alteration of cerebrovascular tone. It can be speculated that the attenuated CBF increase in newborn piglets with IUGR during H/H may also be caused by glucocorticoids. Evidence is available that glucocorticoid activity is increased in fetuses with IUGR because maternal glucocorticoids are insufficiently cleared by the placenta (47,48).

An additional aspect of longer lasting moderate H/H is the observed gradual decline of CBF over time. The amount of reduction was similar between normal-weight piglets and pig-

lets with IUGR (Fig. 1), suggesting that additional IUGR-independent factors affect vasodilatory response during H/H. Opioids are able to provoke a stimulus duration-dependent effect in hypoxic pial artery dilation in newborn pigs. It has been shown that μ -opioid receptors contribute to, whereas κ -opioid receptors oppose, hypoxic pial dilation (49). It is interesting that μ -opioid receptor activation contributes to hypoxic pial dilation during an early period of moderate and severe hypoxia. In contrast, κ -opioid-induced increase of vascular tone became increasingly more important with the longer duration of the stimulus (50). Recent studies indicated direct effects of the endogenous opiate system on brain metabolism after hypoxia/ischemia in newborn piglets (51,52). A gradual CBF reduction caused by compromised cerebral perfusion pressure seems less likely, because nearly all animals exhibit MAP values distinctly above the autoregulatory threshold (44).

A selective decline in CMRO₂ of newborn piglets with IUGR seems to be of substantial interest, because the brain O₂ extraction and CMRO₂-related CBF (CBF divided by CMRO₂) remained similar between normal-weight piglets and piglets with IUGR, but the increased brain lactate production in piglets with IUGR indicates an increased anaerobic cerebral metabolism. Blood *et al.* (53) reported that in the near-term fetal sheep, adenosine mediates a decrease of cerebral metabolic rate during acute moderate hypoxia *via* the adenosine A₁ receptor activation. Furthermore, an inhibition of A₁ receptors during severe asphyxia resulted in an increased neuronal cell death accompanied by delayed suppression of neural activity and increased cerebral metabolism (54). Presently, it is not known whether the fall in CMRO₂ during O₂ deprivation is a result of O₂ starvation or a protective mechanism of adaptive hypometabolism (55,56). However, the mentioned reports strongly suggest that endogenous neuroprotective mechanisms are active in the developing brain. We assume that the presented data of blunted AADC activity and reduced CMRO₂ in the newborn piglets with IUGR during moderate H/H may refer to a further indication of endogenous brain protection against O₂ deprivation.

Acknowledgments. We thank Drs. E. Will and H. Linemann for help during the PET studies and U. Jäger, I. Witte, R. Lücke, R. Herrlich, and L. Wunder for skillful technical assistance.

REFERENCES

- Ashworth A 1998 Effects of intrauterine growth retardation on mortality and morbidity in infants and young children. *Eur J Clin Nutr* 52(suppl 1):S34–S41; discussion S41–S42
- Künzel W, Misselwitz B 2001 [Epidemiology of fetal growth retardation]. *Gynäkologe* 34:784–792
- Levene ML, Kornberg J, Williams TH 1985 The incidence and severity of post-asphyxial encephalopathy in full-term infants. *Early Hum Dev* 11:21–26
- Volpe JJ, Herscovitch P, Perlman JM, Kreusser KL, Raichle ME 1985 Positron emission tomography in the asphyxiated term newborn: parasagittal impairment of cerebral blood flow. *Ann Neurol* 17:287–296
- Vannucci RC 1997 Hypoxic-ischemic encephalopathy: clinical aspects. In: Fanaroff AA, Martin RJ (eds) *Neonatal-Perinatal Medicine. IV*. Mosby-Year Book, Philadelphia, pp 877–891
- Menkes JH, Curran J 1994 Clinical and MR correlates in children with extrapyramidal cerebral palsy. *AJNR Am J Neuroradiol* 15:451–457
- Hoon AH Jr, Reinhardt EM, Kelley RI, Breiter SN, Morton DH, Naidu SB, Johnston MV 1997 Brain magnetic resonance imaging in suspected extrapyramidal cerebral palsy: observations in distinguishing genetic-metabolic from acquired causes. *J Pediatr* 131:240–245
- Roland EH, Poskitt K, Rodriguez E, Lupton BA, Hill A 1998 Perinatal hypoxic-ischemic thalamic injury: clinical features and neuroimaging. *Ann Neurol* 44:161–166
- Johnston MV, Trescher WH, Ishida A, Nakajima W 2001 Neurobiology of hypoxic-ischemic injury in the developing brain. *Pediatr Res* 49:735–741
- Gordon K, Statman D, Johnston MV, Robinson TE, Becker JB, Silverstein FS 1990 Transient hypoxia alters striatal catecholamine metabolism in immature brain: an in vivo microdialysis study. *J Neurochem* 54:605–611
- Nakajima W, Ishida A, Takada G 1996 Effect of anoxia on striatal monoamine metabolism in immature rat brain compared with that of hypoxia: an in vivo microdialysis study. *Brain Res* 740:316–322
- Huang CC, Lajevardi NS, Tammela O, Pastuszko A, Delivoria-Papadopoulos M, Wilson DF 1994 Relationship of extracellular dopamine in striatum of newborn piglets to cortical oxygen pressure. *Neurochem Res* 19:649–655
- Bauer R, Brust P, Walter B, Vorwieger G, Bergmann R, Elhalag E, Fritz A, Steinbach J, Fuchtnier F, Hinz R, Zwiener U, Johannsen B 2002 Effect of hypoxia/hypercapnia on metabolism of 6-[(18F)fluoro-L-DOPA in newborn piglets. *Brain Res* 934:23–33
- Globus MY, Ginsberg MD, Dietrich WD, Busto R, Scheinberg P 1987 Substantia nigra lesion protects against ischemic damage in the striatum. *Neurosci Lett* 80:251–256
- Ren Y, Li X, Xu ZC 1997 Asymmetrical protection of neostriatal neurons against transient forebrain ischemia by unilateral dopamine depletion. *Exp Neurol* 146:250–257
- Bauer R, Walter B, Vorwieger G, Bergmann R, Fuchtnier F, Brust P 2001 Intrauterine growth restriction induces up-regulation of cerebral aromatic amino acid decarboxylase activity in newborn piglets: [18F]fluorodopa positron emission tomographic study. *Pediatr Res* 49:474–480
- Bauer R, Walter B, Hoppe A, Gaser E, Lampe V, Kauf E, Zwiener U 1998 Body weight distribution and organ size in newborn swine (*sus scrofa domestica*)—a study describing an animal model for asymmetrical intrauterine growth retardation. *Exp Toxicol Pathol* 50:59–65
- De Roth L, Downie HG 1976 Evaluation of viability of neonatal swine. *Can Vet J* 17:275–279
- Walter B, Bauer R, Gaser E, Zwiener U 1997 Validation of the multiple colored microsphere technique for regional blood flow measurements in newborn piglets. *Basic Res Cardiol* 92:191–200
- Bauer R, Walter B, Wurker E, Kluge H, Zwiener U 1996 Colored microsphere technique as a new method for quantitative-multiple estimation of regional hepatic and portal blood flow. *Exp Toxicol Pathol* 48:415–420
- Makowski EL, Meschia G, Droegemueller W, Battaglia FC 1968 Measurement of umbilical arterial blood flow to the sheep placenta and fetus in utero. Distribution to cotyledons and the intercotyledonary chorion. *Circ Res* 23:623–631
- Coyle MG, Oh W, Stonestreet BS 1993 Effects of indomethacin on brain blood flow and cerebral metabolism in hypoxic newborn piglets. *Am J Physiol* 264:H141–H149
- Namavari M, Bishop A, Satyamarthy N, Bida G, Barrio JR 1992 Regioselective radiofluorodestannylation with [18F]F2 and [18F]CH₃COOF: a high yield synthesis of 6-[18F]fluoro-L-dopa. *Int J Rad Appl Instrum [A]* 43:989–996
- Brust P, Bauer R, Walter B, Bergmann R, Fuchtnier F, Vorwieger G, Steinbach J, Johannsen B, Zwiener U 1998 Simultaneous measurement of [18F]FDOPA metabolism and cerebral blood flow in newborn piglets. *Int J Dev Neurosci* 16:353–364
- Vorwieger G, Brust P, Bergmann R, Bauer R, Walter B, Fuchtnier F, Steinbach J, Johannsen B 1998 HPLC analysis of the metabolism of 6-[F-18]fluoro-L-DOPA in the brain of neonatal pigs. In: Carson RE, Daube Witherspoon ME, Herscovitch P (eds) *Quantitative Functional Brain Imaging with Positron Emission Tomography*. Academic Press, San Diego, pp 285–292
- Brix G, Zaers J, Adam LE, Bellemann ME, Ostertag H, Trojan H, Haberkorn U, Doll J, Oberdorfer F, Lorenz WJ 1997 Performance evaluation of a whole-body PET scanner using the NEMA protocol. *National Electrical Manufacturers Association. J Nucl Med* 38:1614–1623
- Brust P, Zessin J, Kuwabara H, Pawelke B, Kretzschmar M, Hinz R, Bergman J, Eskola O, Solin O, Steinbach J, Johannsen B 2003 Positron emission tomography imaging of the serotonin transporter in the pig brain using [11C](+)-McN5652 and S-([18F]fluoromethyl)-(+)-McN5652. *Synapse* 47:143–151
- Huang SC, Yu DC, Barrio JR, Grafton S, Melega WP, Hoffman JM, Satyamarthy N, Mazzotta JC, Phelps ME 1991 Kinetics and modeling of L-6-[18F]fluoro-dopa in human positron emission tomographic studies. *J Cereb Blood Flow Metab* 11:898–913
- Cumming P, Gjedde A 1998 Compartmental analysis of dopa decarboxylation in living brain from dynamic positron emission tomograms. *Synapse* 29:37–61
- Eisenhauer CL, Matsuda LS, Ueyehara CF 1994 Normal physiologic values of neonatal pigs and the effects of isoflurane and pentobarbital anesthesia. *Lab Anim Sci* 44:245–252
- Cumming P, Kuwabara H, Ase A, Gjedde A 1995 Regulation of DOPA decarboxylase activity in brain of living rat. *J Neurochem* 65:1381–1390
- Cho S, Neff NH, Hadjiconstantinou M 1997 Regulation of tyrosine hydroxylase and aromatic L-amino acid decarboxylase by dopaminergic drugs. *Eur J Pharmacol* 323:149–157
- Zhu MY, Juorio AV, Paterson IA, Boulton AA 1992 Regulation of aromatic L-amino acid decarboxylase by dopamine receptors in the rat brain. *J Neurochem* 58:636–641
- Zhu MY, Juorio AV, Paterson IA, Boulton AA 1994 Regulation of aromatic L-amino acid decarboxylase in rat striatal synaptosomes: effects of dopamine receptor agonists and antagonists. *Br J Pharmacol* 112:23–30

36. Tammela O, Pastuszko A, Lajevardi NS, Delivoria-Papadopoulos M, Wilson DF 1993 Activity of tyrosine hydroxylase in the striatum of newborn piglets in response to hypocapnic hypoxia. *J Neurochem* 60:1399–1406
37. Hedner T, Lundborg P, Engel J 1978 Effect of hypoxia on monoamine synthesis in brains of developing rats. III. Various O₂ levels. *Biol Neonate* 34:55–60
38. Olano M, Song D, Murphy S, Wilson DF, Pastuszko A 1995 Relationships of dopamine, cortical oxygen pressure, and hydroxyl radicals in brain of newborn piglets during hypoxia and posthypoxic recovery. *J Neurochem* 65:1205–1212
39. Globus MY, Busto R, Dietrich WD, Martinez E, Valdes I, Ginsberg MD 1988 Effect of ischemia on the in vivo release of striatal dopamine, glutamate, and gamma-aminobutyric acid studied by intracerebral microdialysis. *J Neurochem* 51:1455–1464
40. Boksa P, El-Khodori BF 2003 Birth insult interacts with stress at adulthood to alter dopaminergic function in animal models: possible implications for schizophrenia and other disorders. *Neurosci Biobehav Rev* 27:91–101
41. Decker MJ, Hue GE, Caudle WM, Miller GW, Keating GL, Rye DB 2003 Episodic neonatal hypoxia evokes executive dysfunction and regionally specific alterations in markers of dopamine signaling. *Neuroscience* 117:417–425
42. Decker MJ, Rye DB 2002 Neonatal intermittent hypoxia impairs dopamine signaling and executive functioning. *Sleep Breath* 6:205–210
43. Lou HC, Rosa P, Pryds O, Karrebaek H, Lundberg J, Cumming P, Gjedde A 2004 ADHD: increased dopamine receptor availability linked to attention deficit and low neonatal cerebral blood flow. *Dev Med Child Neurol* 46:179–183
44. Bauer R, Walter B, Vollandt R, Zwiener U 2004 Intrauterine growth restriction ameliorates the effects of gradual hemorrhagic hypotension on regional cerebral blood flow and brain oxygen uptake in newborn piglets. *Pediatr Res* 56:639–646
45. Xi Q, Tcheranova D, Parfenova H, Horowitz B, Leffler CW, Jaggar JH 2004 Carbon monoxide activates K_{Ca} channels in newborn arteriole smooth muscle cells by increasing apparent Ca²⁺ sensitivity of alpha-subunits. *Am J Physiol* 286:H610–H618
46. Heinonen K, Fedinec A, Leffler CW 2003 Dexamethasone pretreatment attenuates cerebral vasodilative responses to hypercapnia and augments vasoconstrictive responses to hyperventilation in newborn pigs. *Pediatr Res* 53:260–265
47. Langley-Evans SC, Phillips GJ, Benediktsson R, Gardner DS, Edwards CR, Jackson AA, Seckl JR 1996 Protein intake in pregnancy, placental glucocorticoid metabolism and the programming of hypertension in the rat. *Placenta* 17:169–172
48. Klemcke HG 2000 Dehydrogenase and oxidoreductase activities of porcine placental 11 β -hydroxysteroid dehydrogenase. *Life Sci* 66:1045–1052
49. Armstead WM 1995 Opioids and nitric oxide contribute to hypoxia-induced pial arterial vasodilation in newborn pigs. *Am J Physiol* 268:H226–H232
50. Armstead WM 1998 Role of opioids in hypoxic pial artery dilation is stimulus duration dependent. *Am J Physiol* 275:H861–H867
51. Jagolino AL, Armstead WM 2003 PTK, MAPK, and NOC/oFQ impair hypercapnic cerebrovasodilation after hypoxia/ischemia. *Am J Physiol* 284:H101–H107
52. Philip S, Armstead WM 2003 Newborn pig nociceptin/orphanin FQ activates protein tyrosine kinase and mitogen activated protein kinase to impair NMDA cerebrovasodilation after ischemia. *Neuroreport* 14:201–203
53. Blood AB, Hunter CJ, Power GG 2003 Adenosine mediates decreased cerebral metabolic rate and increased cerebral blood flow during acute moderate hypoxia in the near-term fetal sheep. *J Physiol* 553:935–945
54. Hunter CJ, Bennet L, Power GG, Roelfsema V, Blood AB, Quaedackers JS, George S, Guan J, Gunn AJ 2003 Key neuroprotective role for endogenous adenosine A1 receptor activation during asphyxia in the fetal sheep. *Stroke* 34:2240–2245
55. Hochachka PW, Buck LT, Doll CJ, Land SC 1996 Unifying theory of hypoxia tolerance: molecular/metabolic defense and rescue mechanisms for surviving oxygen lack. *Proc Natl Acad Sci USA* 93:9493–9498
56. Bickler PE, Donohoe PH 2002 Adaptive responses of vertebrate neurons to hypoxia. *J Exp Biol* 205:3579–3586